

1                   **Genome-wide association studies of 27 accelerometry-derived physical activity**  
2                   **measurements identified novel loci and genetic mechanisms**

3  
4   Guanghao Qi,<sup>1†</sup> Diptavo Dutta,<sup>1†</sup> Andrew Leroux,<sup>1,2</sup> Debashree Ray,<sup>1,3</sup> John Muschelli,<sup>1</sup> Ciprian  
5                   Crainiceanu<sup>1</sup> and Nilanjan Chatterjee<sup>1,4\*</sup>

6  
7   <sup>1</sup>Department of Biostatistics, Johns Hopkins Bloomberg School of Public Health, Baltimore, MD  
8   21205, USA

9   <sup>2</sup>Department of Biostatistics and Informatics, University of Colorado, Aurora, CO 80045, USA

10   <sup>3</sup>Department of Epidemiology, Johns Hopkins Bloomberg School of Public Health, Baltimore,  
11   MD 21205, USA

12   <sup>4</sup>Department of Oncology, Johns Hopkins School of Medicine, Baltimore, MD 21205, USA

13

14

15

16

17

18   **This work was supported by an R01 grant from the National Human Genome Research**  
19   **Institute [1 R01 HG010480-01].**

20

21   **†These authors contributed equally to this work**

22   **\*Correspondence to Nilanjan Chatterjee ([nilanjan@jhu.edu](mailto:nilanjan@jhu.edu))**

23 **Abstract**

24

25 Physical inactivity (PA) is an important risk factor for a wide range of diseases. Previous  
26 genome-wide association studies (GWAS), based on self-reported data or a small number of  
27 phenotypes derived from accelerometry, have identified a limited number of genetic loci  
28 associated with habitual PA and provided evidence for involvement of central nervous system  
29 in mediating genetic effects. In this study, we derived 27 PA phenotypes from wrist  
30 accelerometry data obtained from 88,411 UK Biobank study participants. Single-variant  
31 association analysis based on mixed-effects models and transcriptome-wide association studies  
32 (TWAS) together identified 5 novel loci that were not detected by previous studies of PA, sleep  
33 duration and self-reported chronotype. For both novel and previously known loci, we  
34 discovered associations with novel phenotypes including active-to-sedentary transition  
35 probability, light-intensity PA, activity during different times of the day and proxy phenotypes  
36 to sleep and circadian patterns. Follow-up studies including TWAS, colocalization, tissue-specific  
37 heritability enrichment, gene-set enrichment and genetic correlation analyses indicated the  
38 role of the blood and immune system in modulating the genetic effects and a secondary role of  
39 the digestive and endocrine systems. Our findings provided important insights into the genetic  
40 architecture of PA and its underlying mechanisms.

41

42 **Key words:** Genome-wide association studies, physical activity, novel loci, blood and immune  
43 mechanisms

## 44 **Introduction**

45

46 Regular physical activity (PA) is associated with lower risk of a wide range of diseases, including  
47 cancer, diabetes, cardiovascular disease(Kyu et al., 2016), Alzheimer’s disease(Rovio et al.,  
48 2005), as well as mortality(Smirnova et al., 2019; Leroux et al., 2019). However, studies have  
49 indicated that large majority of US adults and adolescents are insufficiently active(Piercy et al.,  
50 2018), and thus PA interventions have great potential to improve public health. PA was shown  
51 to have a substantial genetic component, and understanding its genetic mechanism can inform  
52 the design of individualized interventions(Lightfoot et al., 2018; Moore-Harrison & Lightfoot,  
53 2010). For example, people who are genetically pre-disposed to low PA may benefit more from  
54 early and more frequent guidance.

55

56 A number of previous genome-wide association studies (GWAS) on physical activity have relied  
57 on self-reported phenotypes, which are subject to perception and recall error(De Moor et al.,  
58 2009; Hara et al., 2018; Kim et al., 2014; Klimentidis et al., 2018). Recently, wearable devices  
59 have been used extensively to collect physical activity data objectively and continuously for  
60 multiple days. To date, there have been two GWAS based on accelerometry-derived activity  
61 phenotypes. Both studies used data from the UK Biobank study(Doherty et al., 2017; Bycroft et  
62 al., 2018) but only focused on a few summaries of these high-density PA measurements. One  
63 study considered two accelerometry-derived phenotypes (average acceleration and fraction  
64 accelerations > 425 milli-gravities) and identified 3 loci associated with PA(Klimentidis et al.,  
65 2018). A second study used a machine learning approach to extract PA phenotypes, including

66 overall activity, sleep duration, sedentary time, walking and moderate intensity activity(Doherty  
67 et al., 2018). This study identified 14 loci associated with PA and found that the central nervous  
68 system (CNS) plays an essential role in modulating the genetic effects on PA. However, both  
69 studies used a small number of phenotypes, which may not capture the complexity of PA  
70 patterns.

71  
72 Recent studies suggest that in addition to the total volume of activity, other PA summaries may  
73 be strongly associated with human health and mortality risk. For example, the transition  
74 between active and sedentary states was strongly associated with measures of health and  
75 mortality(Leroux et al., 2019; Schrack et al., 2019). PA relative amplitude, a proxy for sleep  
76 quality and circadian rhythm, was strongly associated with mental health(Rock, Goodwin,  
77 Harmer, & Wulff, 2014a). Moderate-to-vigorous PA (MVPA) and light intensity PA (LIPA) have  
78 also been reported to be associated with health(McGregor, Palarea-Albaladejo, Dall,  
79 Stamatakis, & Chastin, 2019; Young & Haskell, 2018). Thus, there is increasing evidence that  
80 objectively measured PA in the free-living environment is a highly complex phenotype that  
81 requires a large number of summaries that provide complementary information. Understanding  
82 the genetic mechanisms behind these summaries is critical for understanding the genetic  
83 regulation of activity behavior and informing targeted interventions.

84  
85 In this paper, we conducted genome-wide association analysis using 27 accelerometry-derived  
86 PA measurements from UK Biobank data(Bycroft et al., 2018; Doherty et al., 2017). The  
87 phenotypes cover a wide range of features including volumes of activity, activity during

88 different times of the day, active to sedentary transition probabilities, principal components  
89 and proxies for circadian rhythm (**Table 1**). We conducted GWAS using a mixed-model-based  
90 method, fastGWA(Jiang et al., 2019), to identify variants associated with the above phenotypes.  
91 We also conducted transcriptome-wide association studies (TWAS)(Gusev et al., 2016) across  
92 48 tissues to identify genes and tissues harboring the associations. We further conducted  
93 colocalization (Giambartolomei et al., 2014), tissue-specific heritability enrichment(Finucane et  
94 al., 2018; Finucane et al., 2015), gene-set enrichment(Watanabe, Taskesen, van Bochoven, &  
95 Posthuma, 2017) and genetic correlation(Bulik-Sullivan et al., 2015a) analyses to further reveal  
96 the underlying biological mechanisms. We identified 5 novel loci associated with PA and  
97 showed that, in addition to the CNS, blood and immune related mechanisms could play an  
98 important role in modulating the genetic effects on activity, and digestive and endocrine tissues  
99 could play a secondary role.

100

## 101 **Material and Methods**

102

### 103 *Study Cohort and Physical Activity Phenotypes*

104

105 The UK Biobank study consists of ~500,000 individuals in the United Kingdom with  
106 comprehensive genotype and phenotype data(Bycroft et al., 2018). We used a subset of the  
107 103,712 individuals who were invited and agreed to participate in the accelerometry sub-study  
108 where participants wore a wrist-worn accelerometer for up to 7 days(Doherty et al., 2017).  
109 Accelerometry data from participants are available at multiple resolutions. Here, the individual-

110 specific set of accelerometry-based phenotypes was derived from the five-second level  
111 acceleration data provided by the UK Biobank team. We further compressed the data by  
112 averaging the 5-second level data within every minute. Individuals were screened for poor  
113 quality data using indicators provided by the UK Biobank. In addition, we required individuals to  
114 have at least 3 days (12am-12am) of sufficient wear time defined as estimated wear time  
115 greater than 95% of the day ( $\geq 1368$  minutes). Our inclusion criteria for this analysis closely  
116 mirrors that described in a related paper from our group (Leroux et al., 2020) with the exception  
117 that we did not exclude participants younger than 50 at the time of accelerometer wear or  
118 based on missing demographic and lifestyle data and instead excluded individuals based on  
119 ancestry and genotype data (see subsection *Genotype Data* below).

120  
121 Physical activity phenotypes were all calculated at the day level and then averaged within study  
122 participants across days to obtain one measure for each phenotype and study participant. This  
123 led to 31 PA phenotypes for 93,745 study participants that covered a wide spectrum of  
124 information. The phenotypes are described in **Table 1** and briefly summarized as follows: 1)  
125 total volume of activity (total acceleration (TA), total log acceleration (TLA)); 2) activity during  
126 12 disjoint two-hour windows of the day (TLA 12am-2am, TLA 2am-4am, ..., TLA 10pm-12am);  
127 3) duration of sedentary state (ST), LIPA and MVPA; 4) principal components of the log-  
128 transformed minute-level activity profiles (PC1-6); 5) active-to-sedentary transition probability  
129 (ASTP) and sedentary-to-active transition probability (SATP); 6) proxy phenotypes for circadian  
130 patterns, including dynamic activity ratio estimate (DARE), activity during the most active 10  
131 hours (M10) and least active 5 hours (L5) of the day, timing of M10 and L5, and PA relative

132 amplitude  $\left(\frac{M10-L5}{M10+L5}\right)$ . They included most of the phenotypes used in the previous PA association  
133 studies as well (See **Table 1** for details)(Doherty et al., 2018; Klimentidis et al., 2018). The exact  
134 procedure for deriving study participant-specific phenotypes is described in detail in the  
135 supplemental material of the related paper from our group(Leroux et al., 2020). The  
136 phenotypes were inverse-normal transformed

137 
$$INT(y_i) = \Phi^{-1} \left[ \frac{rank(y_i) - k}{n - 2k + 1} \right], \quad k = 3/8,$$

138 where the transformed variables have mean 0 and variance 1.

139

#### 140 Removing Highly Correlated Phenotypes

141

142 Some of the initial 31 PA phenotypes were highly correlated (**Figure S1**). To avoid counting  
143 similar phenotypes multiple times, if two phenotypes had correlation > 0.8 we removed one of  
144 them. First, we removed total acceleration (TA), duration of sedentary state (ST), PC1 and M10  
145 due to their high correlation with total log acceleration (TLA). TLA was retained as the main  
146 metric for the total volume of activity. Since two previous GWASs used TA as the main metric  
147 for the volume of activity (Doherty et al., 2018; Klimentidis et al., 2018), we chose TLA instead  
148 of TA to avoid repetition with existing work. In addition, the original distribution of TA is highly  
149 skewed, which may not be completely addressed by the INT. In total, 4 phenotypes were  
150 removed and 27 PA phenotypes were retained for the association analysis.

151

#### 152 Genotype Data

153

154 The imputed genotype data for ~93 million variants, using UK10K, 1000 Genomes (Phase 3) and  
155 Haplotype Reference Consortium as reference panel, provided by UK Biobank were used and  
156 merged with the PA phenotype data. Following the Neale lab UK Biobank GWAS pipeline  
157 ([https://github.com/Nealelab/UK\\_Biobank\\_GWAS/blob/master/imputed-v2-  
158 gwas/README.md](https://github.com/Nealelab/UK_Biobank_GWAS/blob/master/imputed-v2-gwas/README.md)), we excluded study participants according to the following criteria: 1) non-  
159 white ancestry; 2) putative sex chromosome aneuploidy; 3) an excessive number of relatives  
160 (more than 10 putative third-degree relatives in the kinship table); 4) sample was not in the  
161 input for phasing of chr1-chr22. After applying these exclusion criteria the sample was further  
162 reduced to 88,411 study participants for downstream analysis.

163

164 We conducted variant quality control to ensure that genetic variants with poor genotyping  
165 quality do not affect the results. Specifically, variants that satisfy any of the following criteria  
166 were removed: 1) imputation INFO score < 0.8; 2) MAF < 0.01; 3) Hardy-Weinberg Equilibrium  
167 (HWE)  $p$ -value <  $1 \times 10^{-6}$ ; 4) missing in more than 10% study participants. After the filtering,  
168 8,951,705 variants remained for downstream analysis, of which 8,067,228 (90.1%) were single  
169 nucleotide polymorphisms (SNPs) and the rest (9.9%) were insertion-deletions (INDELs).

170

### 171 Association Analysis

172

173 We used a fast mixed-effects model method, fastGWA(Jiang et al., 2019), for genome-wide  
174 association analysis. Like other mixed-effects model methods, fastGWA allows the inclusion of  
175 related and unrelated individuals but improves computational efficiency by incorporating a



176 sparse genetic relationship matrix (GRM). The GRM measures the genetic similarity between  
177 individuals and each element is the correlation of genotypes between a pair of individuals. We  
178 constructed the GRM using linkage disequilibrium (LD)-pruned variants that had MAF > 5% and  
179 were present in HapMap3 (LD-pruning was done in PLINK using the following set up as  
180 recommended in Jiang et al (Jiang et al., 2019): window size = 1000Kb, step-size = 100 and  $r^2 =$   
181 0.9). We further computed a sparse-GRM at sparsity level 0.05 to capture the genetic  
182 relatedness between the closely related individuals only and reduced others to zero. We used  
183 the Haseman-Elston regression to estimate the variance of the random effects as an  
184 intermediate step of fastGWA. This approach is orders of magnitude faster than the previous  
185 state-of-the-art, BOLT-LMM(Loh et al., 2015; Loh, Kichaev, Gazal, Schoech, & Price, 2018).  
186  
187 Models were adjusted for age, sex and the first 20 genetic principal components as covariates.  
188 Because the PA phenotypes are correlated, principal component analysis (PCA) was conducted  
189 on the phenotypes to estimate the number of independent phenotypes before setting the  
190 GWAS significance threshold. At least 19 phenotype PCs were needed to explain 99% percent of  
191 the PA phenotypic variance (**Figure S2**). Variants with p-value below the threshold  
192  $5 \times 10^{-8}/19 = 2.63 \times 10^{-9}$  were declared to be statistically significant, which accounted for  
193 the number of independent phenotypes. LD clumping was conducted based on the minimum p-  
194 value across phenotypes. The requirements for the lead SNPs of different loci were to have  
195  $r^2 < 0.1$  and be at least > 500kb apart.  
196

197 A locus was defined as novel if its lead variant is >500kb from the lead variant of any known loci  
198 discovered by the following GWASs on PA, sleep, and circadian rhythm: (1) Doherty et al study  
199 on a smaller set of accelerometry-derived PA phenotypes(Doherty et al., 2018); (2) Klimentidis  
200 et al study on self-reported and accelerometry-derived PA(Klimentidis et al., 2018); (3) Dashti et  
201 al study on self-reported sleep duration(Dashti et al., 2019); (4) Jones et al study on circadian  
202 rhythm(Jones et al., 2019). Considering the diversity of PA phenotypes, we further ensure these  
203 loci do not have associations with other related traits not listed above, by searching for the lead  
204 variants in Open Targets Genetics (OTG, <https://genetics.opentargets.org/>). A locus remains  
205 novel if the lead variant: 1) is not associated at  $p < 5 \times 10^{-8}$  with traits whose names include  
206 the following keywords: accelerometry, physical, exercise, sleep, nap, circadian and  
207 chronotype; 2) and is not in LD with previously reported GWAS lead variants for these traits  
208 ( $r^2 > 0.5$ ).

209  
210 Transcriptome-wide association studies (TWAS) were conducted using the FUSION R  
211 program(Gusev et al., 2016) with reference models generated from 48 tissues of GTEx v7(GTEx  
212 et al., 2017). TWAS analysis was limited to the 18 traits with at least one genome-wide  
213 significant variant ( $p < 2.63 \times 10^{-9}$ ). Multiple testing due to the large number of tissue-trait  
214 combinations ( $48 \times 18 = 864$ ) was addressed by a two-stage adjustment approach: 1) for each  
215 variant, the Benjamini-Hochberg (BH) adjustment was applied across all tissue-trait pairs; 2)  
216 each variant with BH-adjusted p-value  $2.5 \times 10^{-6}$  was then identified (accounting for 20,000  
217 protein-coding genes). Since there can be multiple genes in close proximity to each other, to  
218 identify independent loci detected by TWAS analysis, genes were clustered based on significant

219 associations. A clumping approach was used, which selected the gene with the smallest  
220 minimum p-value across tissue-trait pairs and removed the other genes with a transcription  
221 start site (TSS) within 1Mb of the lead gene TSS. The process continued by identifying the gene  
222 with the next smallest minimum p-value and iterating. The only exception was when the lead  
223 gene of the cluster was not a protein-coding gene (e.g., pseudogene, lncRNA) and a protein-  
224 coding gene was in the cluster. In this case the protein-coding gene with the smallest minimum  
225 p-value was identified as the lead gene. This led to independent gene clusters at genomic loci  
226 which were least 1Mb apart, i.e., none of the lead gene TSS is within the cis region of another  
227 lead gene.

228

### 229 Enrichment Analysis

230

231 Stratified LD score regression(Finucane et al., 2015; Finucane et al., 2018) was used to identify  
232 the tissues and genomic annotations enriched by the heritability for PA. For tissue specific  
233 analysis, chromatin-based annotations were used as derived from the ENCODE and Roadmap  
234 data(ENCODE, 2012; Roadmap et al., 2015) by Finucane et al(Finucane et al., 2018). The  
235 annotations were based on narrow peaks of DNase I hypersensitivity site (DHS) and five  
236 activating histone marks (H3K27ac, H3K4me3, H3K4me1, H3K9ac and H3K36me3) observed for  
237 111 tissues or cell types, resulting in a total of 489 annotations. Stratified LD score regression  
238 computes the heritability attributed to each annotation and computes a coefficient and a p-  
239 value that characterize enrichment.

240

241 In a separate analysis, the enrichment of TWAS signals was evaluated among the genes that  
242 have been reported to be associated to different traits, using FUMA(Watanabe et al., 2017;  
243 Watanabe, Umićević Mirkov, de Leeuw, van den Heuvel, & Posthuma, 2019). For a given PA  
244 trait, we defined a gene-set as the genes that were significant at an exome-wide level ( $p <$   
245  $2.5 \times 10^{-6}$ ) and investigated whether these genes overlapped with the genes that have been  
246 mapped to genome-wide significant variants for different traits as reported in GWAS  
247 catalog(Buniello et al., 2019). The collection of such genes have been detailed in Molecular  
248 Signatures Database (MSigDB)(Liberzon et al., 2011). We used FUMA to compute the  
249 proportion of genes related to other diseases and traits that were also identified by our TWAS  
250 analysis and computed enrichment p-values using the Fisher's exact test.

251

### 252 Colocalization Analysis

253

254 For each susceptibility locus of PA (**Table 2**), colocalization analysis was conducted between its  
255 most significantly associated phenotype and eQTL effects on gene expression in 48 tissues in  
256 GTEx v7(GTEx et al., 2017). SNPs within +-200kb radius of the lead SNP were used and genes  
257 that had at least one significant eQTL (q-value < 0.05) in the region were considered. Analysis  
258 was conducted using the R package COLOC (Giambartolomei et al., 2014) and GWAS and eQTL  
259 effects were identified as being colocalized if PP4 > 0.8.

260

### 261 Heritability and Genetic Correlation Analysis

262

263 Heritability of activity phenotypes was estimated using Haseman-Elston regression as an  
264 intermediate output of fastGWA(Jiang et al., 2019). Our fastGWA analysis computed sparse  
265 GRM at sparsity level 0.05 as recommended by the fastGWA paper (see “Association analysis”).  
266 However, this cutoff may miss the subtle relatedness in the sample and affect heritability  
267 estimate. As a sensitivity analysis, we re-estimated the heritability using a lower sparsity  
268 threshold at 0.02 to capture more subtle relatedness. The genetic correlation between 18 PA  
269 traits and 238 complex traits and diseases was estimated using LD score regression(Bulik-  
270 Sullivan et al., 2015a) implemented in LD Hub(Zheng et al., 2017). In particular, we focused on  
271 four broad groups of traits and diseases (A) cholesterol levels (B) anthropometric traits (C)  
272 autoimmune disease and (D) miscellaneous traits including psychiatric, neurological, cognitive  
273 and personality traits. For each trait and within each category, we applied a false discovery rate  
274 correction to the p-values corresponding to the genetic correlation estimated using LD score  
275 regression, to account for multiple testing. Any genetic correlation with FDR-adjusted p-value  
276 less than 10% were declared as significant.

277

## 278 **Results**

279

### 280 *Genetic Loci Associated with Physical Activity*

281

282 Single-variant genome-wide association analysis identified a total of 16 independent loci,  
283 including three novel ones compared to previous studies (**Table 2 and Figure 1**). All three novel  
284 loci were discovered on chromosome 3: the locus indexed by rs3836464 was associated with

285 ASTP; the locus indexed by rs9818758 was associated with relative amplitude, which is a proxy  
286 sleep behavior and circadian rhythm(Rock, Goodwin, Harmer, & Wulff, 2014b); the locus  
287 indexed by indel 3:131647162\_TA\_T (no rsid available) was associated with TLA 2am-4am  
288 which is a proxy phenotype for activity during sleep. LIPA appeared to be associated with other  
289 SNPs near 3:131647162\_TA\_T but not the lead variant itself, indicating multiple independent  
290 signals at the same locus (**Figure 1**). Nearest coding genes for the novel loci include *SEC13*,  
291 *USP4*, and *CPNE4*.

292  
293 Our analysis also identified novel phenotypes for several known loci (**Table 2**). The strongest  
294 signal was seen for the locus indexed by rs113851554 which is associated with multiple sleep  
295 and circadian rhythm proxy phenotypes including TLA 12am-2am ( $p = 6.7 \times 10^{-37}$ ), TLA 2am-  
296 4am ( $p = 7.9 \times 10^{-39}$ ), average log acceleration during the least active 5 hours of the day (L5,  
297  $p = 1.3 \times 10^{-33}$ ), timing of L5 ( $p = 5.4 \times 10^{-22}$ ) and PA relative amplitude ( $p = 6.9 \times 10^{-15}$ ).  
298 This locus was previously identified to be associated with accelerometry-derived sleep duration  
299 in UK Biobank(Doherty et al., 2018). Among other known loci, 5 were only discovered in the  
300 GWAS of self-reported circadian rhythm(Jones et al., 2019) but not in the other studies  
301 considered (**Table 2**, last column). In our analysis, the loci indexed by rs1144566, rs9369062 and  
302 rs12927162 were associated with sleep proxy phenotypes including timing of L5, TLA 12am-  
303 2am, TLA 2am-4am and TLA 10pm-12am. Three other loci, indexed by rs301799, rs2909950 and  
304 rs12717867, were associated with TLA 6pm-8pm and LIPA, respectively.

305

306 In addition to the phenotypic associations above, other variants in some of the loci captured  
307 associations that are not reflected by the lead variants. In particular, variants in high LD with  
308 rs2138543 are associated with a wide range of phenotypes including LIPA, MVPA, activity  
309 during two-hour windows, and a number of proxy phenotypes for circadian patterns (**Table S1**).

310

### 311 Transcriptome-Wide Association Study and Colocalization Analysis

312

313 We performed transcriptome-wide association studies (TWAS) (Gamazon et al., 2015; Gusev et  
314 al., 2016) for each PA trait based on gene expression data across 48 tissues available through  
315 GTEx (version 7)(GTEx et al., 2017). Our analysis identified 15 loci (**Table 3, Figure 2, Table S2**)  
316 with significant association in at least one trait-tissue pair analysis after correcting for multiple  
317 testing (Benjamini-Hochberg corrected p-value  $< 2.5 \times 10^{-6}$ , see **Methods**). We identified two  
318 novel loci. One of them was indexed by *RN7SKP16*, whose higher expression in brain putamen  
319 basal ganglia is genetically associated with lower level of MVPA. Another was indexed by  
320 pseudogene *PDXDC2P (16q22.1)*, whose higher expression in esophagus mucosa and EBV  
321 transformed lymphocytes appeared to be genetically associated with lower level of TLA 6am-  
322 8am (**Figure 2**). See **Table S2** for details of these associations. These loci was not previously  
323 reported by any prior GWAS and were not close to any of the 3 novel regions detected by our  
324 single variants analysis (**Table 3**).

325

326 The TWAS analysis also identified novel PA phenotypes, potential target genes and underlying  
327 tissues for many of the known loci or novel loci detected through single variant analysis (**Table**

328 **3**). Consistent with a previous study (Doherty et al., 2018), the TWAS analysis showed that  
329 genetic association for PA traits often points towards involvement of CNS (**Table 3**). Further, our  
330 analysis indicates consistent involvement of blood and immune, digestive and endocrine  
331 systems in modulating the genetic effects on PA. See **Table S2** for a complete list of associated  
332 tissues. Among the 15 loci significant in TWAS analysis, the lead genes of 4 loci were  
333 significantly associated with PA phenotypes via the blood and immune tissues. For example, the  
334 genetically predicted expression of *PBX3* and *KANSL1* in the blood and immune tissues (whole  
335 blood, EBV-transformed lymphocytes) were each associated with 3 PA phenotypes. The genes  
336 associated with PA via blood and immune tissues were also associated via digestive (esophagus  
337 mucosa, small intestine - terminal ileum, colon – sigmoid, etc) and/or endocrine (thyroid,  
338 pituitary) tissues, but only one of them overlapped with the 9 genes that were associated with  
339 PA phenotypes through the CNS (**Table 3**). Another locus, represented by *C3orf62*, were  
340 associated with PA relative amplitude only via the digestive and endocrine tissues (esophagus  
341 mucosa, colon – sigmoid, thyroid) but not the blood/immune tissues or CNS. These findings  
342 suggested two potential pathways for the genetic regulation of PA: a primary pathway involving  
343 the CNS (brain in particular) and a secondary pathway involving the blood/immune system and,  
344 potentially, the digestive and endocrine systems. The actual biological processes involved in the  
345 pathways are beyond the scope of this paper and may be worth future investigation.

346  
347 Several genes that were found to be significantly associated to specific PA traits in our TWAS  
348 analysis, were also found to be highly overlapping with genes that were previously reported to  
349 be associated with various traits and diseases including but not limited to neuropsychiatric



350 diseases, behavioral traits, anthropometric traits and autoimmune diseases (**Figure S3**). For  
351 example, we found that the genes associated with TLA across different tissues, are enriched for  
352 genes that have been associated with neuroticism, bipolar disorder, Parkinson's disease,  
353 cognitive function and several others indicating the putative involvement of the CNS in the  
354 genetic mechanism of TLA. Additionally, the genes associated with relative amplitude  
355 overlapped highly with those associated with several autoimmune diseases like inflammatory  
356 bowel disease, ulcerative colitis in addition to different behavioral and cognitive traits (**Figure**  
357 **S3**). These results further supported the possible involvement of both CNS as well as the blood  
358 and immune system in the genetic mechanism of PA traits.

359  
360 We performed a colocalization analysis to gain further insights on the tissue specific activity of  
361 the significant genetic loci. Among the 16 loci significantly associated with PA, 9 loci colocalized  
362 with the eQTL signals for at least one gene and one tissue with a colocalization probability  
363 ( $PP4$ )  $> 0.8$  (**Table S3**). Colocalization occurred in a similar set of tissues as those that harbored  
364 the TWAS associations (**Table 3 and Table S3**), namely the CNS, blood and immune (whole  
365 blood, spleen, EBV transformed lymphocytes), digestive (esophagus, colon) and endocrine  
366 (thyroid, testis, adrenal gland) tissues, and also in a number of cardiovascular tissues that were  
367 not highlighted by TWAS. Among the 15 lead genes for TWAS significant loci, the eQTL signal of  
368 4 genes (*RERE*, *C3orf62*, *PBX3* and *RP11-396F22.1*) colocalized with PA GWAS signal in at least  
369 one tissue. Colocalization also occurred in two other secondary genes (*RP5-1115A15.1* and  
370 *CASC10*).

371

372 *Analysis of Heritability and Co-Heritability*

373

374 Our fastGWA analysis estimated genome-wide heritability of PA phenotypes as an intermediate  
375 output. The estimates appeared to be dependent on the sparsity level of the genetic  
376 relationship matrix (**Figure S4**). We chose the results under the lower cutoff (0.02) since it  
377 captured more subtle relatedness and should give more accurate heritability estimates. The  
378 estimates of heritability varied across different PA phenotypes. A number of traits were  
379 estimated to have higher heritability than others, including TLA (0.15), TLA 6pm-8pm (0.15),  
380 MVPA (0.14) (**Figure S4**). Afternoon and pre-sleep evening activity (TLA 4pm to 12am) appeared  
381 to be more heritable than morning activity (TLA 2am to 12pm). As could be expected,  
382 phenotypes with higher heritability tend to have a higher average  $\chi^2$  statistic for genetic  
383 associations, and a QQ plot which deviate further from the null line (**Figure S5**). The magnitude  
384 of heritability estimates was generally consistent with previous studies, which reported 10-20%  
385 heritability for PA traits (Doherty et al., 2018; Klimentidis et al., 2018). We also notice that  
386 heritability estimated using restricted maximum likelihood (REML) tended to be slightly higher  
387 Haseman-Elston regression estimates (**Figure S4**).

388

389 We further used stratified LD-score regression for partitioning heritability by functional  
390 annotations of genome (Finucane et al., 2015; Finucane et al., 2018). Consistent with TWAS  
391 findings, this analysis also indicated possible role for blood and immune system in addition to  
392 CNS for genetic regulation of PA (**Figure 3**). In particular, heritabilities for both TLA and LIPA  
393 were enriched for DNase I hypersensitivity sites (DHS) in primary B cells from peripheral blood

394 and that for TLA 12pm-2pm were enriched for H3K27ac in spleen. We also found potential  
395 enrichment in other traits, though they were not significant after FDR adjustment. For example,  
396 for TLA 8am-10am, MVPA, and ASTP the heritability enrichment in active chromatin regions of  
397 blood/immune tissues were all close to being statistically significant (**Figure S6**).

398  
399 We further used LD score regression(Bulik-Sullivan et al., 2015a; Bulik-Sullivan et al., 2015b) to  
400 explore genetic correlation between PA phenotypes and four broad groups of complex traits  
401 and diseases (**Figure S7**). Genetic correlations were identified (FDR < 10%) between PA  
402 phenotypes and: (1) neurological, psychiatric and cognitive traits, including Alzheimer's disease  
403 (AD), attention-deficit hyperactivity disorder (ADHD), depressive symptoms, intelligence, and  
404 neo-conscientiousness; (2) auto-immune diseases, with the strongest correlation for multiple  
405 sclerosis and weaker correlations for Crohn's disease and primary biliary cirrhosis; (3) obesity-  
406 related anthropometric traits and (4) cholesterol levels. Most PA traits have negative genetic  
407 correlation with obesity-related traits and triglycerides, and positive genetic correlation with  
408 HDL cholesterol. The directions of genetic correlation with the other two categories of traits are  
409 mixed (**Figure S7**). These results broadly supported our previous results indicating the role of  
410 CNS and blood/immune related mechanisms in the genetics of PA traits.

411

## 412 **Discussion**

413

414 In summary, our study provided novel insights to genetic architecture of physical activity  
415 through genome-wide association analysis of an extensive set of accelerometry based PA

416 phenotypes, derived in the UK biobank study, and a series of follow-up genomic analyses. We  
417 identified a total of six novel loci, most of which were associated with PA phenotypes not  
418 considered in previous studies (Dashti et al., 2019; Doherty et al., 2018; Jones et al., 2019;  
419 Klimentidis et al., 2018). Our analysis also identified novel phenotypes associated with the  
420 known loci. Further, we provided multiple independent lines of evidence that genetic  
421 mechanisms for association for PA involve the blood and immune system.

422

423 Compared to the 15 loci identified by the two previous GWASs on accelerometry-based PA  
424 (Doherty et al., 2018; Klimentidis et al., 2018), the novel loci we discovered have increased the  
425 number of PA susceptibility loci by 33%. Most of the novel loci were connected to the  
426 expression of genes, pseudogenes or long non-coding RNAs (lncRNA, **Table 2 and 3**), and  
427 *C3orf62* was also supported by evidence of colocalization (**Table S3**). The novel locus indexed by  
428 rs9818758 overlaps with the TWAS locus index by *C3orf62*. Though it was unclear how *C3orf62*  
429 is involved in PA, two secondary genes in the locus, *ARIH2* and *DAG1* (**Table 3**), appeared to be  
430 involved in the following biological processes: *ARIH2* was found to be essential for  
431 embryogenesis by regulating the immune system (Lin et al., 2013); *DAG1* was found to play a  
432 role in the regeneration of skeletal muscles (Cohn et al., 2002). Both processes appeared  
433 relevant for PA. We argue that the two loci above, supported by multiple lines of evidence  
434 including GWAS, TWAS, colocalization and gene functions, should be prioritized in follow-up  
435 studies. Another two novel loci were connected to pseudogene *RN7SKP16* and *PDXDC2P* of  
436 which the function is less clear and may also be worth future investigation. However, Dashti et  
437 al found a transcription factor site variant rs915416 to be associated with sleep duration, which

438 is approximately 930Kb away from the transcription start site of *RN7SKP1* and might have  
439 potential long range regulatory effects which warrants further study. Among the genes located  
440 in known loci, *PBX3* and *RP11-396F22.1* were highlighted by both TWAS and colocalization  
441 results. *PBX3* is a member of the pre-B cell leukemia (PBX) family which have extensive roles in  
442 early development and some adult processes (Morgan & Pandha, 2020), which could also  
443 modulate its association with PA.

444  
445 The novel phenotypes in this study provided important insights into the genetic architecture of  
446 PA, which may have been overlooked by previous GWASs on a small number of phenotypes.  
447 The accelerometry-based study by Doherty et al identified the genetic associations with overall  
448 activity, sleep duration and sedentary time(Doherty et al., 2018); the study by Klimentidis et al  
449 studied the average acceleration and the duration of active states(Klimentidis et al., 2018). Our  
450 results found that there can be different genetic architecture for PA during different times of  
451 the day, and there can be unique variants that only affect certain PA patterns, like ASTP, LIPA  
452 and relative amplitude, but not others (**Table 2**). The heritability and genetic correlation can  
453 also vary across different PA phenotypes (**Figures S4 and S7**).

454  
455 TWAS and tissue-specific heritability enrichment analysis suggested that in addition to the CNS,  
456 the blood and immune system could be also associated with PA. This finding was further  
457 supported by colocalization, gene-set enrichment and genetic correlation analyses. A previous  
458 study(Doherty et al., 2018), which explored enrichment of heritability for PA traits by tissue-  
459 specific gene expression patterns, identified potential modulating role of the CNS,

460 adrenal/pancreatic and skeletal muscle tissues. Our study, which used a more extended set of  
461 phenotypes and chromatin-state-based annotations, confirmed previous findings and further  
462 highlighted the role of the blood and immune system. Though there is lack of studies on the  
463 effect of immune functions on PA, previous medical literature has established the effect of PA  
464 on immune functions. A study showed that higher PA is associated with elevation of T-  
465 regulatory cells and lower risk for autoimmune diseases(Sharif et al., 2018). Multiple studies  
466 showed that regular moderately intense PA boost immune functions in older adults and  
467 protects against age-related inflammatory disorders(Dhalwani et al., 2016; Duggal, Niemi, and  
468 Harridge, Simpson, & Lord, 2019; Vancampfort et al., 2017). Though the direction of causal  
469 effect may not be the same as that suggested by genetic analyses, these studies supported  
470 broad connections between PA and immune functions. Future studies are needed to better  
471 understand the underlying mechanisms and causal directions.

472  
473 In addition to the blood and immune system, TWAS and enrichment analysis also suggested  
474 that the digestive system and endocrine system could be involved in modulating the genetic  
475 effects on PA. The literature has also established broad connections between PA and digestive  
476 and endocrine tissues. A previous study found that PA has complex effects on gastrointestinal  
477 health(Peters, De Vries, Vanberge-Henegouwen, & Akkermans, 2001): acute strenuous activity  
478 may provoke gastrointestinal symptoms while low-intensity activity could have benefits.  
479 Interestingly, three TWAS loci that were significant in digestive tissues were associated with PA  
480 phenotypes that are proxies for meal-time activity: *PDXDC2P* with TLA 6am-8am, *RERE* with TLA  
481 6pm-8PM and *KANSL1* with TLA 4pm-6pm (**Table 3**). It was also known that multiple organs in

482 the endocrine system produce hormones that regulate physiological functions of the body,  
483 which can have complex bidirectional relationships with PA(Ciloglu et al., 2005; Hawkins et al.,  
484 2008; Ennour-Idrissi, Maunsell, & Diorio, 2015; Alessa et al., 2017; Hackney & Saeidi, 2019).  
485 Among the endocrine tissues, thyroid appeared to be modulating the genetic effect of the  
486 largest number of loci. Previous studies showed that TWAS lead genes *PBX3*, *Corf62* and  
487 *KANSL1* were highly expressed in thyroid (GTEx et al., 2017), and SNPs near *KANSL1* were found  
488 to be associated with thyroid-stimulating hormone levels (Teumer et al., 2018). Our TWAS  
489 analysis indicated that the genes associated with PA via the blood and immune system tended  
490 to also be associated with the digestive and endocrine systems, but do not usually overlap with  
491 the genes associated with the CNS. This suggests that the blood and immune, digestive and  
492 endocrine systems may be involved in the same broad pathway that affects PA, which is  
493 different from that of CNS.

494

495 It is noteworthy that the accelerometry-derived PA phenotypes in this study are not limited to  
496 exercise, but include a variety of broad-sense activity patterns. In fact, we do find that several  
497 phenotypes have strong genetic correlation with sleep, chronotype and other behavioral traits  
498 (**Figure S7**). Therefore, when defining novel loci, we have further excluded those variants  
499 previously reported to be associated with PA, sleep and circadian rhythm. However, due to the  
500 nature of accelerometry, which captures the acceleration of human body, those phenotypes  
501 are still essentially and broadly PA phenotypes, though they can indirectly reflect and be related  
502 to other traits. Hence we still address all of them by PA phenotypes throughout the paper.

503

504 This study has a number of limitations. Though we derived a more extensive set of PA  
505 phenotypes than previous studies, information was still lost when collapsing a 7-day continuous  
506 times series of wrist accelerometry into 31 PA phenotypes. The ideal approach would be to  
507 conduct a GWAS utilizing all the information across the 7 days of accelerometry measurements.  
508 Results could outline genetic regulation of a continuous course of PA over time. The current  
509 analysis of TLA during 12 non-overlapping two-hour time intervals during the day, indicated  
510 that different genetic variants may affect PA during different times of the day (**Tables 2 and 3**).  
511 Another limitation is that some of the phenotypes are not directly interpretable. For example,  
512 the PCs of log acceleration are less interpretable than other phenotypes, such as TLA and ASTP.  
513 However, they do reflect important features of physical activity and warrant further  
514 investigations. A potential solution is to obtain proxy measurements that are interpretable and  
515 highly correlated with PC scores.

516

517 In conclusion, we conducted association studies on a wide range of PA phenotypes and  
518 identified 5 novel loci associated with PA. We found that in addition to the CNS, the blood and  
519 immune system may also play an important role in the genetic mechanisms of PA, and the  
520 digestive and endocrine systems could also be involved in the blood and immune pathway.

521

## 522 **Data Availability**

523 Data supporting the findings of this paper are available upon application to the UK Biobank  
524 study. The summary statistics are publicly available via the GWAS Catalog  
525 (<https://www.ebi.ac.uk/gwas/>) under accession numbers GCST90061408-GCST90061434.



526

## 527 **Supplemental Data**

528 Supplemental Data include seven figures and four tables.

529

## 530 **Declaration of Interests**

531 Dr. Ciprian Crainiceanu is consulting with Bayer and Johnson and Johnson on methods  
532 development for wearable devices in clinical trials. The details of the contracts are disclosed  
533 through the Johns Hopkins University eDisclose system and have no direct or apparent  
534 relationship with the current paper. The other authors declare no conflict of interest.

535

## 536 **Acknowledgements**

537 The UK Biobank data was accessed via application ID 17712. Research of Drs. Guanghao Qi,  
538 Diptavo Dutta and Nilanjan Chatterjee was supported by an R01 grant from the National  
539 Human Genome Research Institute [1 R01 HG010480-01].

540

## 541 **Web Resources**

542

543 UK Biobank: <https://www.ukbiobank.ac.uk/>

544 fastGWA software: <https://cnsgenomics.com/software/gcta/#fastGWA>

545 FUSION TWAS software: <http://gusevlab.org/projects/fusion/>

546 COLOC R package: <https://cran.r-project.org/web/packages/coloc/index.html>

547 LD score regression software: <https://github.com/bulik/ldsc>

548 LD Hub: <http://ldsc.broadinstitute.org/ldhub/>  
549 FUMA GWAS: <https://fuma.ctglab.nl/>  
550 PLINK: <https://www.cog-genomics.org/plink/2.0/>  
551 Molecular Signatures Database: <http://www.broadinstitute.org/msigdb>  
552 Open Targets Genetics: <https://genetics.opentargets.org/>

553

## 554 **References**

555

556 Alessa, H. B., Chomistek, A. K., Hankinson, S. E., Barnett, J. B., Rood, J., Matthews, C.  
557 E., . . . Tobias, D. K. (2017). Objective Measures of Physical Activity and Cardiometabolic  
558 and Endocrine Biomarkers. *Med Sci Sports Exerc*, *49*(9), 1817-1825.  
559 doi:10.1249/MSS.0000000000001287

560 Bulik-Sullivan, B., Finucane, H. K., Anttila, V., Gusev, A., Day, F. R., Loh, P. R., . . . Neale, B. M.  
561 (2015a). An atlas of genetic correlations across human diseases and traits. *Nature*  
562 *Genetics*, *47*(11), 1236-1241. doi:10.1038/ng.3406

563 Bulik-Sullivan, B. K., Loh, P. R., Finucane, H. K., Ripke, S., Yang, J., Schizophrenia Working Group  
564 of the Psychiatric Genomics Consortium, . . . Neale, B. M. (2015b). LD Score regression  
565 distinguishes confounding from polygenicity in genome-wide association studies. *Nature*  
566 *Genetics*, *47*(3), 291-295. doi:10.1038/ng.3211

567 Buniello, A., MacArthur, J. A. L., Cerezo, M., Harris, L. W., Hayhurst, J., Malangone,  
568 C., . . . Parkinson, H. (2019). The NHGRI-EBI GWAS Catalog of published genome-wide

569 association studies, targeted arrays and summary statistics 2019. *Nucleic Acids Research*,  
570 47(D1), D1005-D1012. doi:10.1093/nar/gky1120

571 Bycroft, C., Freeman, C., Petkova, D., Band, G., Elliott, L. T., Sharp, K., . . . Marchini, J. (2018). The  
572 UK Biobank resource with deep phenotyping and genomic data. *Nature*, 562(7726), 203-  
573 209. doi:10.1038/s41586-018-0579-z

574 Ciloglu, F., Peker, I., Pehlivan, A., Karacabey, K., Ilhan, N., Saygin, O., & Ozmerdivenli, R. (2005).  
575 Exercise intensity and its effects on thyroid hormones. *Neuro Endocrinol Lett*, 26(6), 830-  
576 834. Retrieved from <https://www.ncbi.nlm.nih.gov/pubmed/16380698>

577 Cohn, R. D., Henry, M. D., Michele, D. E., Barresi, R., Saito, F., Moore, S. A., . . . Campbell, K. P.  
578 (2002). Disruption of DAG1 in differentiated skeletal muscle reveals a role for dystroglycan  
579 in muscle regeneration. *Cell*, 110(5), 639-648. doi:10.1016/s0092-8674(02)00907-8

580 Dashti, H. S., Jones, S. E., Wood, A. R., Lane, J. M., van Hees, V. T., Wang, H., . . . Saxena, R.  
581 (2019). Genome-wide association study identifies genetic loci for self-reported habitual  
582 sleep duration supported by accelerometer-derived estimates. *Nature Communications*,  
583 10(1), 1100. doi:10.1038/s41467-019-08917-4

584 De Moor, M. H., Liu, Y. J., Boomsma, D. I., Li, J., Hamilton, J. J., Hottenga, J. J., . . . Deng, H. W.  
585 (2009). Genome-wide association study of exercise behavior in Dutch and American  
586 adults. *Med Sci Sports Exerc*, 41(10), 1887-1895. doi:10.1249/MSS.0b013e3181a2f646

587 Dhalwani, N. N., O'Donovan, G., Zaccardi, F., Hamer, M., Yates, T., Davies, M., & Khunti, K.  
588 (2016). Long terms trends of multimorbidity and association with physical activity in older  
589 English population. *Int J Behav Nutr Phys Act*, 13, 8. doi:10.1186/s12966-016-0330-9

- 590 Doherty, A., Jackson, D., Hammerla, N., Plötz, T., Olivier, P., Granat, M. H., . . . Wareham, N. J.  
591 (2017). Large Scale Population Assessment of Physical Activity Using Wrist Worn  
592 Accelerometers: The UK Biobank Study. *PLoS One*, *12*(2), e0169649.  
593 doi:10.1371/journal.pone.0169649
- 594 Doherty, A., Smith-Byrne, K., Ferreira, T., Holmes, M. V., Holmes, C., Pulit, S. L., & Lindgren, C.  
595 M. (2018). GWAS identifies 14 loci for device-measured physical activity and sleep  
596 duration. *Nature Communications*, *9*(1), 5257. doi:10.1038/s41467-018-07743-4
- 597 Duggal, N. A., Niemi, G., Harridge, S. D. R., Simpson, R. J., & Lord, J. M. (2019). Can physical  
598 activity ameliorate immunosenescence and thereby reduce age-related multi-morbidity.  
599 *Nat Rev Immunol*, *19*(9), 563-572. doi:10.1038/s41577-019-0177-9
- 600 ENCODE Project Consortium (2012). An integrated encyclopedia of DNA elements in the human  
601 genome. *Nature*, *489*(7414), 57-74. doi:10.1038/nature11247
- 602 Ennour-Idrissi, K., Maunsell, E., & Diorio, C. (2015). Effect of physical activity on sex hormones in  
603 women: a systematic review and meta-analysis of randomized controlled trials. *Breast  
604 Cancer Res*, *17*(1), 139. doi:10.1186/s13058-015-0647-3
- 605 Finucane, H. K., Bulik-Sullivan, B., Gusev, A., Trynka, G., Reshef, Y., Loh, P. R., . . . Price, A. L.  
606 (2015). Partitioning heritability by functional annotation using genome-wide association  
607 summary statistics. *Nature Genetics*, *47*(11), 1228-1235. doi:10.1038/ng.3404
- 608 Finucane, H. K., Reshef, Y. A., Anttila, V., Slowikowski, K., Gusev, A., Byrnes, A., . . . Price, A. L.  
609 (2018). Heritability enrichment of specifically expressed genes identifies disease-relevant  
610 tissues and cell types. *Nature Genetics*, *50*(4), 621-629. doi:10.1038/s41588-018-0081-4

611 Gamazon, E. R., Wheeler, H. E., Shah, K. P., Mozaffari, S. V., Aquino-Michaels, K., Carroll, R.  
612 J., . . . Im, H. K. (2015). A gene-based association method for mapping traits using  
613 reference transcriptome data. *Nature Genetics*, *47*(9), 1091-1098. doi:10.1038/ng.3367  
614 Giambartolomei, C., Vukcevic, D., Schadt, E. E., Franke, L., Hingorani, A. D., Wallace, C., &  
615 Plagnol, V. (2014). Bayesian test for colocalisation between pairs of genetic association  
616 studies using summary statistics. *PLoS Genetics*, *10*(5), e1004383.  
617 doi:10.1371/journal.pgen.1004383  
618 GTEx Consortium (2017). Genetic effects on gene expression across human tissues. *Nature*,  
619 *550*(7675), 204-213. doi:10.1038/nature24277  
620 Gusev, A., Ko, A., Shi, H., Bhatia, G., Chung, W., Penninx, B. W., . . . Pasaniuc, B. (2016).  
621 Integrative approaches for large-scale transcriptome-wide association studies. *Nature*  
622 *Genetics*, *48*(3), 245-252. doi:10.1038/ng.3506  
623 Hackney, A. C., & Saeidi, A. (2019). The thyroid axis, prolactin, and exercise in humans. *Curr*  
624 *Opin Endocr Metab Res*, *9*, 45-50. doi:10.1016/j.coemr.2019.06.012  
625 Hara, M., Hachiya, T., Sutoh, Y., Matsuo, K., Nishida, Y., Shimano, C., . . . Wakai, K. (2018).  
626 Genomewide Association Study of Leisure-Time Exercise Behavior in Japanese Adults.  
627 *Med Sci Sports Exerc*, *50*(12), 2433-2441. doi:10.1249/MSS.0000000000001712  
628 Hawkins, V. N., Foster-Schubert, K., Chubak, J., Sorensen, B., Ulrich, C. M., Stanczyk, F.  
629 Z., . . . McTiernan, A. (2008). Effect of exercise on serum sex hormones in men: a 12-  
630 month randomized clinical trial. *Med Sci Sports Exerc*, *40*(2), 223-233.  
631 doi:10.1249/mss.0b013e31815bbba9

- 632 Jiang, L., Zheng, Z., Qi, T., Kemper, K. E., Wray, N. R., Visscher, P. M., & Yang, J. (2019). A  
633 resource-efficient tool for mixed model association analysis of large-scale data. *Nature*  
634 *Genetics*, *51*(12), 1749-1755. doi:10.1038/s41588-019-0530-8
- 635 Jones, S. E., Lane, J. M., Wood, A. R., van Hees, V. T., Tyrrell, J., Beaumont, R. N., . . . Weedon,  
636 M. N. (2019). Genome-wide association analyses of chronotype in 697,828 individuals  
637 provides insights into circadian rhythms. *Nature Communications*, *10*(1), 343.  
638 doi:10.1038/s41467-018-08259-7
- 639 Kim, J., Min, H., Oh, S., Kim, Y., Lee, A. H., & Park, T. (2014). Joint identification of genetic  
640 variants for physical activity in Korean population. *Int J Mol Sci*, *15*(7), 12407-12421.  
641 doi:10.3390/ijms150712407
- 642 Klimentidis, Y. C., Raichlen, D. A., Bea, J., Garcia, D. O., Wineinger, N. E., Mandarino, L.  
643 J., . . . Going, S. B. (2018). Genome-wide association study of habitual physical activity in  
644 over 377,000 UK Biobank participants identifies multiple variants including CADM2 and  
645 APOE. *Int J Obes (Lond)*, *42*(6), 1161-1176. doi:10.1038/s41366-018-0120-3
- 646 Kyu, H. H., Bachman, V. F., Alexander, L. T., Mumford, J. E., Afshin, A., Estep, K., . . . Forouzanfar,  
647 M. H. (2016). Physical activity and risk of breast cancer, colon cancer, diabetes, ischemic  
648 heart disease, and ischemic stroke events: systematic review and dose-response meta-  
649 analysis for the Global Burden of Disease Study 2013. *BMJ*, *354*, i3857.  
650 doi:10.1136/bmj.i3857
- 651 Leroux, A., Di, J., Smirnova, E., MCGuffey, E. J., Cao, Q., Bayatmokhtari, E., . . . Crainiceanu, C.  
652 (2019). Organizing and analyzing the activity data in NHANES. *Stat Biosci*, *11*(2), 262-287.  
653 doi:10.1007/s12561-018-09229-9

- 654 Leroux, A., Xu, S., Kundu, P., Muschelli, J., Smirnova, E., Chatterjee, N., & Crainiceanu, C. (2020).  
655 Quantifying the Predictive Performance of Objectively Measured Physical Activity on  
656 Mortality in the UK Biobank. *J Gerontol A Biol Sci Med Sci*. doi:10.1093/gerona/glaa250
- 657 Liberzon, A., Subramanian, A., Pinchback, R., Thorvaldsdóttir, H., Tamayo, P., & Mesirov, J. P.  
658 (2011). Molecular signatures database (MSigDB) 3.0. *Bioinformatics*, 27(12), 1739-1740.  
659 doi:10.1093/bioinformatics/btr260
- 660 Lightfoot, J. T., DE Geus, E. J. C., Booth, F. W., Bray, M. S., DEN Hoed, M., Kaprio,  
661 J., . . . Bouchard, C. (2018). Biological/Genetic Regulation of Physical Activity Level:  
662 Consensus from GenBioPAC. *Med Sci Sports Exerc*, 50(4), 863-873.  
663 doi:10.1249/MSS.0000000000001499
- 664 Lin, A. E., Ebert, G., Ow, Y., Preston, S. P., Toe, J. G., Cooney, J. P., . . . Pellegrini, M. (2013).  
665 ARIH2 is essential for embryogenesis, and its hematopoietic deficiency causes lethal  
666 activation of the immune system. *Nature Immunology*, 14(1), 27-33. doi:10.1038/ni.2478
- 667 Loh, P. R., Kichaev, G., Gazal, S., Schoech, A. P., & Price, A. L. (2018). Mixed-model association  
668 for biobank-scale datasets. *Nature Genetics*, 50(7), 906-908. doi:10.1038/s41588-018-  
669 0144-6
- 670 Loh, P. R., Tucker, G., Bulik-Sullivan, B. K., Vilhjálmsson, B. J., Finucane, H. K., Salem, R.  
671 M., . . . Price, A. L. (2015). Efficient Bayesian mixed-model analysis increases association  
672 power in large cohorts. *Nature Genetics*, 47(3), 284-290. doi:10.1038/ng.3190
- 673 McGregor, D. E., Palarea-Albaladejo, J., Dall, P. M., Stamatakis, E., & Chastin, S. F. M. (2019).  
674 Differences in physical activity time-use composition associated with cardiometabolic  
675 risks. *Prev Med Rep*, 13, 23-29. doi:10.1016/j.pmedr.2018.11.006

- 676 Moore-Harrison, T., & Lightfoot, J. T. (2010). Driven to be inactive? The genetics of physical  
677 activity. *Prog Mol Biol Transl Sci*, *94*, 271-290. doi:10.1016/B978-0-12-375003-7.00010-8
- 678 Morgan, R., & Pandha, H. S. (2020). PBX3 in Cancer. *Cancers (Basel)*, *12*(2).  
679 doi:10.3390/cancers12020431
- 680 Peters, H. P., De Vries, W. R., Vanberge-Henegouwen, G. P., & Akkermans, L. M. (2001).  
681 Potential benefits and hazards of physical activity and exercise on the gastrointestinal  
682 tract. *Gut*, *48*(3), 435-439. doi:10.1136/gut.48.3.435
- 683 Piercy, K. L., Troiano, R. P., Ballard, R. M., Carlson, S. A., Fulton, J. E., Galuska, D. A., . . . Olson, R.  
684 D. (2018). The Physical Activity Guidelines for Americans. *JAMA*, *320*(19), 2020-2028.  
685 doi:10.1001/jama.2018.14854
- 686 Roadmap, E. C., Kundaje, A., Meuleman, W., Ernst, J., Bilenky, M., Yen, A., . . . Kellis, M. (2015).  
687 Integrative analysis of 111 reference human epigenomes. *Nature*, *518*(7539), 317-330.  
688 doi:10.1038/nature14248
- 689 Rock, P., Goodwin, G., Harmer, C., & Wulff, K. (2014a). Daily rest-activity patterns in the bipolar  
690 phenotype: A controlled actigraphy study. *Chronobiol Int*, *31*(2), 290-296.  
691 doi:10.3109/07420528.2013.843542
- 692 Rock, P., Goodwin, G., Harmer, C., & Wulff, K. (2014b). Daily rest-activity patterns in the bipolar  
693 phenotype: A controlled actigraphy study. *Chronobiol Int*, *31*(2), 290-296.  
694 doi:10.3109/07420528.2013.843542
- 695 Rovio, S., Kåreholt, I., Helkala, E. L., Viitanen, M., Winblad, B., Tuomilehto, J., . . . Kivipelto, M.  
696 (2005). Leisure-time physical activity at midlife and the risk of dementia and Alzheimer's  
697 disease. *Lancet Neurol*, *4*(11), 705-711. doi:10.1016/S1474-4422(05)70198-8



- 698 Schrack, J. A., Kuo, P. L., Wanigatunga, A. A., Di, J., Simonsick, E. M., Spira, A. P., . . . Zipunnikov,  
699 V. (2019). Active-to-Sedentary Behavior Transitions, Fatigability, and Physical Functioning  
700 in Older Adults. *J Gerontol A Biol Sci Med Sci*, *74*(4), 560-567. doi:10.1093/gerona/gly243
- 701 Sharif, K., Watad, A., Bragazzi, N. L., Lichtbroun, M., Amital, H., & Shoenfeld, Y. (2018). Physical  
702 activity and autoimmune diseases: Get moving and manage the disease. *Autoimmun Rev*,  
703 *17*(1), 53-72. doi:10.1016/j.autrev.2017.11.010
- 704 Smirnova, E., Leroux, A., Cao, Q., Tabacu, L., Zipunnikov, V., Crainiceanu, C., & Urbanek, J.  
705 (2019). The predictive performance of objective measures of physical activity derived  
706 from accelerometry data for 5-year all-cause mortality in older adults: NHANES 2003-  
707 2006. *J Gerontol A Biol Sci Med Sci*. doi:10.1093/gerona/glz193
- 708 Teumer, A., Chaker, L., Groeneweg, S., Li, Y., Di Munno, C., Barbieri, C., . . . Medici, M. (2018).  
709 Genome-wide analyses identify a role for SLC17A4 and AADAT in thyroid hormone  
710 regulation. *Nature Communications*, *9*(1), 4455. doi:10.1038/s41467-018-06356-1
- 711 Vancampfort, D., Koyanagi, A., Ward, P. B., Rosenbaum, S., Schuch, F. B., Mugisha,  
712 J., . . . Stubbs, B. (2017). Chronic physical conditions, multimorbidity and physical activity  
713 across 46 low- and middle-income countries. *Int J Behav Nutr Phys Act*, *14*(1), 6.  
714 doi:10.1186/s12966-017-0463-5
- 715 Watanabe, K., Taskesen, E., van Bochoven, A., & Posthuma, D. (2017). Functional mapping and  
716 annotation of genetic associations with FUMA. *Nature Communications*, *8*(1), 1826.  
717 doi:10.1038/s41467-017-01261-5

718 Watanabe, K., Umićević Mirkov, M., de Leeuw, C. A., van den Heuvel, M. P., & Posthuma, D.  
719 (2019). Genetic mapping of cell type specificity for complex traits. *Nature*  
720 *Communications*, 10(1), 3222. doi:10.1038/s41467-019-11181-1

721 Young, D. R., & Haskell, W. L. (2018). Accumulation of Moderate-to-Vigorous Physical Activity  
722 and All-Cause Mortality. *J Am Heart Assoc*, 7(6). doi:10.1161/JAHA.118.008929

723 Zheng, J., Erzurumluoglu, A. M., Elsworth, B. L., Kemp, J. P., Howe, L., Haycock, P. C., . . . Neale,  
724 B. M. (2017). LD Hub: a centralized database and web interface to perform LD score  
725 regression that maximizes the potential of summary level GWAS data for SNP heritability  
726 and genetic correlation analysis. *Bioinformatics*, 33(2), 272-279.  
727 doi:10.1093/bioinformatics/btw613

728

729

730

**Table 1. Description of physical activity phenotypes.**

Category	Phenotype abbreviation	Phenotype full name and description
Total volume of activity	TA*	Total acceleration.
	TLA	Total log acceleration. Sum of $\log(1+\text{acceleration})$ .
Activity during 2-hour windows of the day	TLA 12am-2am, TLA 2am-4am, TLA 4am-6pm, ..., TLA 8pm-10pm, TLA 10pm-12am	Total log acceleration in the k-th two-hour window of the day, starting from midnight (12 intervals in total)
Duration of activity patterns	ST*	Duration of sedentary state. Time when the acceleration is less than 30 milli-gravity (mg) is defined as sedentary state.
	LIPA	Duration of light-intensity physical activity (LIPA). LIPA is defined as the time when the acceleration is $\geq 30\text{mg}$ but $< 100\text{mg}$ .
	MVPA	Duration of moderate to vigorous physical activity (MVPA). MVPA is defined as the time when the acceleration is $\geq 100\text{mg}$ .
Principal components	PC1*, PC2, ..., PC6	First 6 principal component of the log-transformed minute-level activity profiles.
Active-sedentary transition patterns	SATP	Sedentary to active transition probability. SATP is the probability of transitioning to active state if the subject is currently sedentary. Active state is defined as acceleration $\geq 30\text{mg}$ and sedentary state is defined as acceleration $< 30\text{mg}$ .
	ASTP	Active to sedentary transition probability. SATP is the probability of transitioning to sedentary state if the subject is currently active.
Circadian rhythm proxies	DARE	Dynamic activity ratio estimate. Total log-acceleration during 8am-8pm as proportion of TLA for the whole day.
	M10*	Average log acceleration during the ten most active hours of the day
	L5	Average log acceleration during the five least active hours of the day
	Timing of M10	Mid-point of the ten most active hours of the day
	Timing of L5	Mid-point of the five least active hours of the day
	Relative amplitude	Relative amplitude = $(M10-L5)/(M10+L5)$ . It measures the difference between daytime activity and activity during sleep.

All the phenotypes are first calculated at the day level and then averaged across 7 days.

\* Excluded from genetic association analyses due to high correlation ( $>0.8$ ) with TLA.

**Table 2. Significant loci associated with physical activity in single-variant analysis.**

Lead variant <sup>a</sup>	Chromosome region	Base pair	Minor allele	Major allele	Minor allele frequency	Nearest coding gene and distance <sup>d</sup>	Significantly associated traits <sup>c</sup>	Previous studies that discovered the locus
Novel loci <sup>b</sup>								
rs3836464	3p25.3	10454772	CA	C	0.274	SEC13 (92kb)	ASTP (p=2.2e-09, b=-0.032)	NA
rs9818758	3p21.31	49382925	A	G	0.171	USP4 (4.8kb)	Relative amplitude (p=2.1e-09, b=-0.036)	
3:131647162_TA_T	3q22	131647162	T	TA	0.466	CPNE4 (357kb)	TLA 2am-4am (p=2.2e-09, b=0.029)	
Known loci								
rs1144566	1q25.3	182569626	T	C	0.030	RGS16 (3.9kb)	Timing of L5 (p=5e-10, b=-0.086)*	4
rs301799	1p36.23	8489302	C	T	0.422	SLC45A1 (111kb)	TLA 6pm-8pm (p=1.7e-09, b=0.027)*	OTG <sup>e</sup>
rs113851554	2p14	66750564	T	G	0.050	MEIS1 (90kb)	TLA 12am-2am (p=6.7e-37, b=0.138)*, TLA 2am-4am (p=7.9e-39, b=0.142)*, L5 (p=1.3e-33, b=0.13)*, Relative amplitude (p=6.9e-15, b=-0.082)*, Timing of L5 (p=5.4e-22, b=0.105)*	1,4
rs2909950	5q33.1	151886147	A	G	0.418	NMUR2 (73kb)	TLA 6pm-8pm (p=9.4e-10, b=-0.028)*	4
rs12717867	5q33.1	152412845	G	A	0.453	GRIA1 (456kb)	LIPA (p=6.2e-10, b=-0.029)*	4
rs9369062	6p21.2	38437303	C	A	0.292	BTBD9 (171kb)	TLA 12am-2am (p=1.5e-12, b=-0.037)*, TLA 2am-4am (p=2.3e-10, b=-0.033)*	4
rs2006810	7q11.22	69902152	C	T	0.395	GALNT17 (695kb)	TLA 8pm-10pm (p=8.1e-11, b=-0.031)*	1,4
rs1268539	9q33.3	128195657	A	C	0.419	GAPVD1 (172kb)	TLA (p=1.1e-10, b=0.03), LIPA (p=3.2e-10, b=0.03)*	1
rs564819152	10p12.31	21820650	G	A	0.320	SKIDA1 (5kb)	TLA 8am-10am (p=1.4e-09, b=-0.031)*	1,3
rs2138543	12q12	39298423	A	T	0.477	CPNE8 (2.8kb)	TLA 6am-8am (p=3.9e-11, b=0.03)*, PC2 (p=1.5e-09, b=-0.029)*	4
rs12927162	16q12.2	52684916	G	A	0.277	TOX3 (103kb)	TLA 10pm-12am (p=1e-09, b=0.032)*	4
rs2532402	17q21.31	44304130	G	C	0.221	KANSL1 (1.4kb)	TLA (p=1.5e-12, b=0.04), MVPA (p=1.9e-10, b=0.035)	1,2,3,4
rs3837946	19p13.2	9955920	TTTGT	T	0.475	PIN1 (10kb)	TLA (p=1.3e-11, b=-0.032), LIPA (p=1.6e-09, b=-0.029)*	1,3

<sup>a</sup>Significant variants (single nucleotide polymorphism (SNP) or insertion/deletion) are defined as those with fastGWA p-value <  $2.63 \times 10^{-9}$  (Bonferroni corrected for 19 independent traits). LD clumping was performed at  $r^2 < 0.1$  and lead variants of different loci were required to be >500kb apart.

<sup>b</sup>A locus is defined as novel if its lead variant is >500kb from the lead variant of any loci identified in one of the previous GWAS: 1) Doherty et al study on a smaller set of accelerometry-based physical activity; 2) Klimentidis et al study on self-reported and accelerometry based physical activity; 3) Dashti et al study on self-reported sleep duration; 4) Jones et al study on circadian rhythm. Loci that were discovered by the four above studies are marked with 1, 2, 3 and 4 in the last column, respectively. Novel phenotypes associated with known loci are marked with \*.

<sup>c</sup>Traits are followed by p-values (p) and effect sizes (b). The effects size b is for the effect of minor allele vs major allele, e.g. a positive b indicates the minor allele is the trait-increasing allele. TLA: total log-acceleration. ASTP: active-to-sedentary transition probability. MVPA: moderate-to-vigorous physical activity. PC2: second principal component. LIPA: light-intensity physical activity.

<sup>d</sup>Nearest coding gene is defined as the protein-coding gene whose transcription start site (TSS) is closest to the variant.

<sup>e</sup>This locus was not reported by the four studies we catalogued but was associated with daytime nap, as reported by Open Targets Genetics (OTG). See Table S4 for details.

**Table 3. Significant loci associated with physical activity identified in transcriptome-wide association studies (TWAS).**

Most significant gene <sup>a</sup>	CHR	Gene start	Gene end	Locus	Minimum p-value across traits and tissues	Secondary genes in the locus with comparable associations <sup>c</sup>	Trait and tissue <sup>d</sup>	Previous studies that discovered the locus
Novel loci <sup>b</sup>								
<i>RN7SKP16</i>	1	33802167	33802465	1p35.1	2.72E-09	-	MVPA (CNS)	
<i>PDXDC2P</i>	16	70069541	70098679	16q22.1	1.81E-09	-	TLA 6am-8am (Blood/Immune, Digestive)	NA
Known loci								
<i>RERE</i> <sup>†</sup>	1	8412457	8877702	1p36.23	5.28E-09	<i>ENO1-IT1, RP5-1115A15.1</i> <sup>†</sup>	TLA 6pm-8pm (Digestive, Other, Blood/Immune)	GWAS
<i>RP5-1160K1.6</i>	1	110171118	110171939	1p13.3	7.68E-10	-	PC2 (CNS)	4
<i>C3orf62</i> <sup>†</sup>	3	49306219	49315263	3p21.31	3.28E-10	<i>RP11-694I15.7, ARIH2, DAG1, SLC25A20</i>	Relative amplitude (Digestive, Endocrine)	GWAS
<i>CTC-467M3.3</i>	5	87988462	87989789	5q14.3	1.39E-08	-	ASTP (CNS)	1,4
<i>NMUR2</i>	5	151771093	151812929	5q33.1	8.88E-10	-	TLA 6pm-8pm (CNS, Other)	4, GWAS
<i>PBX3</i> <sup>†</sup>	9	128509624	128729656	9q33.3	3.04E-10	<i>MAPKAP1</i>	LIPA (Blood/Immune, Digestive, Endocrine, Other); SATP (Blood/Immune, Other, Digestive, Endocrine); TLA (Blood/Immune, Other, Digestive, Endocrine)	1, GWAS
<i>DNAJC1</i>	10	22045466	22292698	10p12.31	3.20E-09	<i>CASC10</i> <sup>†</sup>	TLA 8am-10am (CNS)	1,3, GWAS
<i>RP11-396F22.1</i> <sup>†</sup>	12	39300253	39303394	12q12	9.89E-10	-	Timing of M10 (CNS), PC2 (CNS, Other), TLA 6am-8am (CNS, Other)	4, GWAS
<i>FMNL1</i>	17	43299590	43324633	17q21.31	2.82E-09	<i>CTD-2020K17.1</i>	TLA (CNS)	1,4
<i>KANSL1</i>	17	44107282	44302733	17q21.31	2.17E-13	<i>KANSL1-AS1, RP11-798G7.8</i>	MVPA (CNS, Blood/Immune, Other, Digestive, Musculoskeletal/connective); TLA 4pm-6pm (Blood/Immune, Other, Digestive); TLA (Adipose, CNS, Blood/Immune, Other, Digestive, Cardiovascular, Musculoskeletal/connective, Endocrine)	1,2,3,4, GWAS
<i>ZNF846</i>	19	9862669	9903856	19p13.2	2.22E-10	<i>OLFM2, PIN1, CTD-2623N2.3</i>	TLA (Other)	1,3, GWAS
<i>JUND</i>	19	18390563	18392432	19p13.11	3.18E-09	-	SATP (Other)	4
<i>LINC00634</i>	22	42348169	42354937	22q13.2	4.85E-11	-	TLA (CNS)	4

<sup>a</sup>For each gene, we apply Benjamini-Hochberg (BH) correction across all trait-tissue pairs. Significant genes are defined as those with BH corrected p-value <  $2.5 \times 10^{-6}$ . Significant genes are clustered using an approach similar to LD clumping so that different loci, marked by the transcription start site (TSS) of the lead gene, are >1Mb apart. Gene symbols are italicized. <sup>†</sup> Genes of which the eQTL signal colocalizes with GWAS signal of the most significantly associated phenotype.

<sup>b</sup>A locus is defined as novel if its flanking region ( $\pm 500$ kb from TSS) does not harbor a variant reported in Table 2 or any of the four previous studies considered in Table 2. Loci that were discovered by the above studies are marked with 1, 2, 3 and 4 in the last column, respectively. Loci that were discovered by our single-variant analysis (Table 2) are marked with "GWAS" in the first column.

<sup>c</sup>Other genes in the cluster with minimum p-value less than 10 times the minimum p-value of the lead gene are shown in column "Secondary genes in the locus with comparable associations". See Table S2 for all the significant tissue-trait pairs.

<sup>d</sup>CNS: central nervous system. TLA: total log-acceleration. ASTP: active-to-sedentary transition probability. SATP: sedentary-to-active transition probability. MVPA: moderate-to-vigorous physical activity. PC2: second principal component.

## Figures

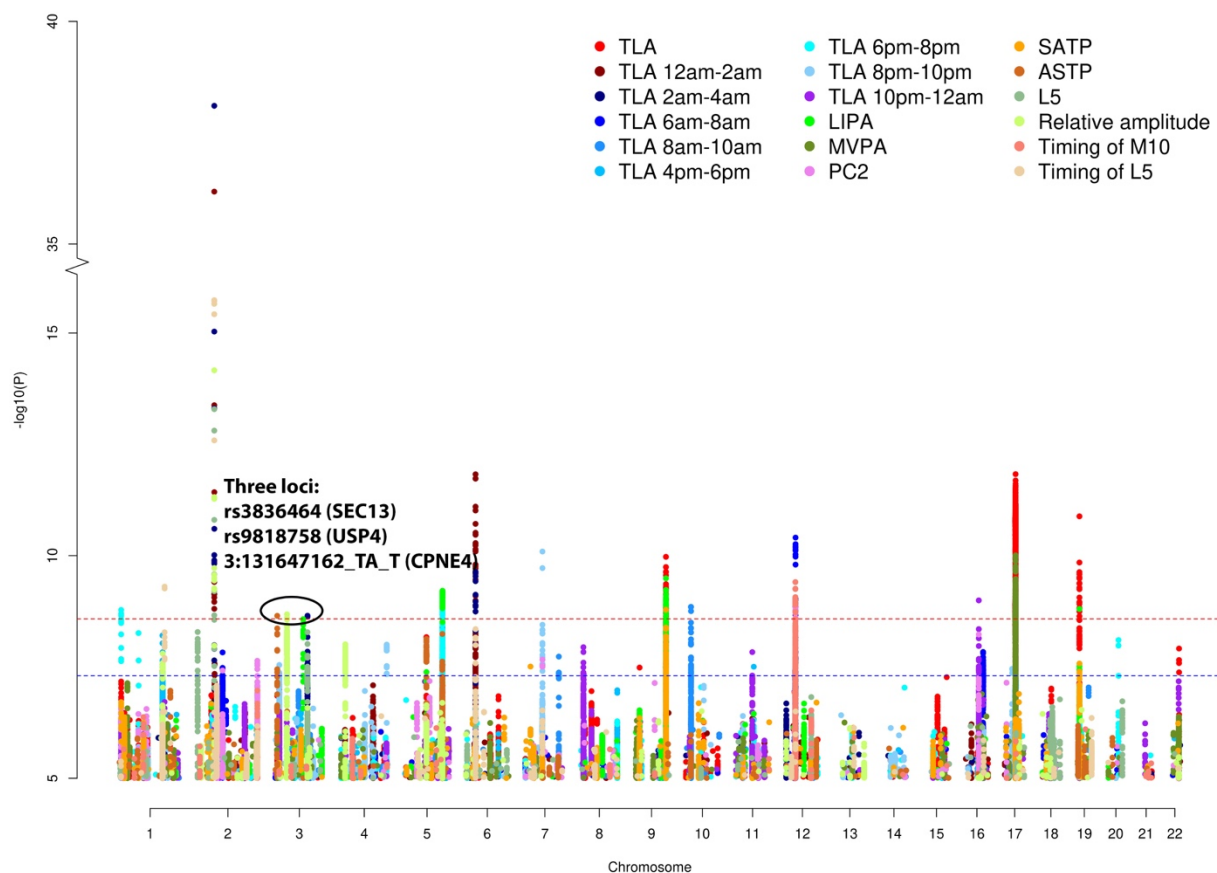
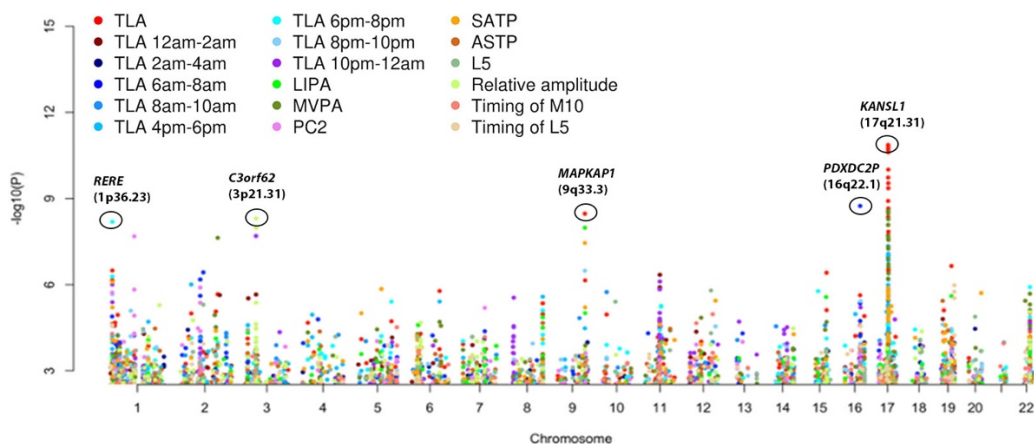
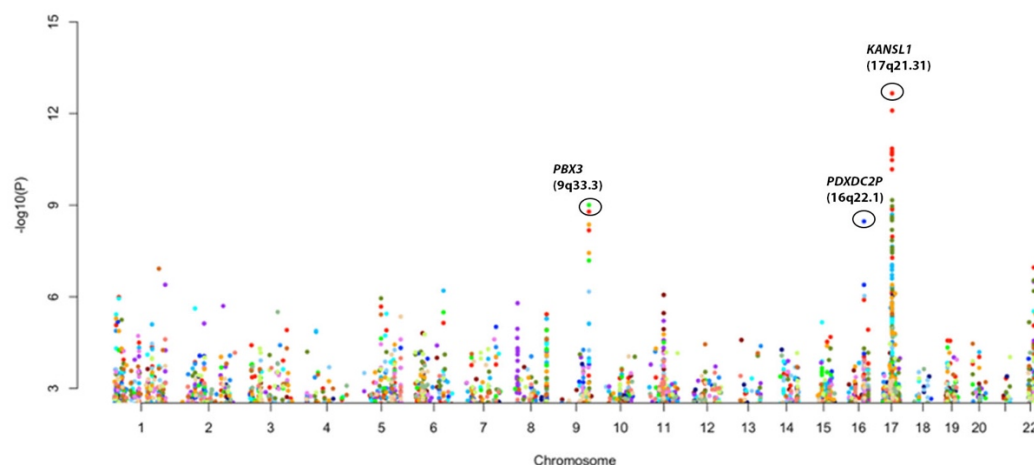


**Figure 1. Manhattan plot for 18 traits that are significantly associated with at least one variant at  $p < 2.63 \times 10^{-9}$  in single-variant analysis.** The red dashed line is  $p = 2.63 \times 10^{-9}$  accounting for the number of independent traits. The blue dashed line is the standard genome-wide significance threshold  $p = 5 \times 10^{-8}$ . Three novel loci that have not been discovered in previous GWAS of physical activity, sleep duration and circadian rhythm are circled out and annotated by the lead variant and nearest coding gene (see Table 2).

**(a) Esophagus mucosa**



**(b) Cells - EBV-transformed lymphocytes**



**(c) Brain putamen basal ganglia**

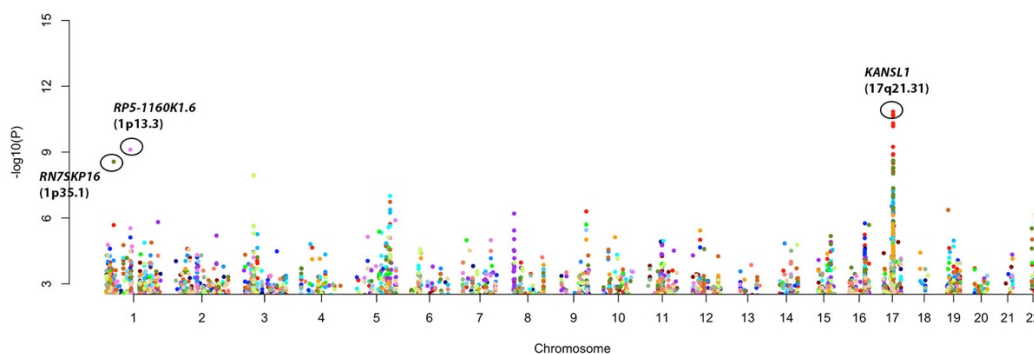


**Figure 2: TWAS Manhattan plots for three tissues that harbor the TWAS novel loci.** Significant genes with FDR corrected  $p$ -values  $< 2.5 \times 10^{-6}$  are circled (see Methods for details). Only the PA traits that are significantly associated with at least one variant at  $p < 2.63 \times 10^{-9}$  in single-variant analysis are shown.

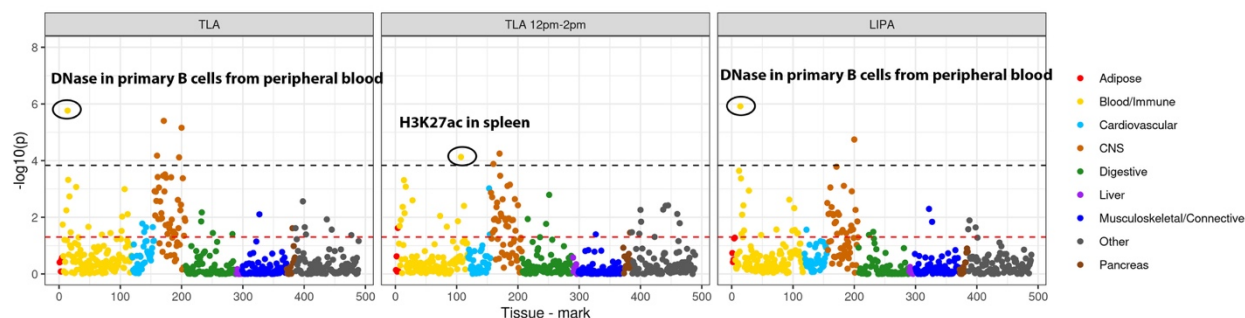


**Figure 3. Tissue-specific heritability enrichment p-values for traits with significant enrichment at FDR < 0.05 in blood and immune tissues.** The analysis was conducted using tissue/cell type specific stratified LD score regression based on 6 chromatin-based annotations in 111 tissues and cell types described in Finucane et al, Nature Genetics 2018 (PMID: 29632380). Each dot corresponds to an annotation in a tissue or cell type. A complete list of tissue and cell types is provided in Supplementary Table 7 of the above paper. Black line corresponds to FDR < 0.05 ( $-\log(p\text{-value})=3.83$ ) across all combinations of trait, tissue, and histone mark. Red line corresponds to  $p = 0.05$ . See Figure S6 for the enrichment p-values for the rest of the traits. CNS: central nervous system.